Chapter 5

Spreading Code Acquisition and Tracking

No matter which form of spread spectrum technique we employ, we need to have the timing information of the transmitted signal in order to despread the received signal and demodulate the despread signal. For a DS-SS system, we see from the discussions in Chapters 2 and 3 that if we are off even by a single chip duration, we will be unable to despread the received spread spectrum signal, since the spread sequence is designed to have a small out-of-phase autocorrelation magnitude. Therefore, the process of acquiring the timing information of the transmitted spread spectrum signal is essential to the implementation of any form of spread spectrum technique.

Usually the problem of timing acquisition is solved via a two-step approach:

- *Initial code acquisition (coarse acquisition or coarse synchronization)* which synchronizes the transmitter and receiver to within an uncertainty of $\pm Tc$
- *Code tracking* which performs and maintains fine synchronization between the transmitter and receiver.

Given the initial acquisition, code tracking is a relatively easy task and is usually accomplished by a delay lock loop (DLL). The tracking loop keeps on operating during the whole communication period. If the channel changes abruptly, the delay lock loop will lose track of the correct timing and initial acquisition will be re-performed. Sometimes, we perform initial code acquisition periodically no matter whether the tracking loop loses track or not.

Compared to code tracking, initial code acquisition in a spread spectrum system is usually very

difficult. First, the timing uncertainty, which is basically determined by the transmission time of the transmitter and the propagation delay, can be much longer than a chip duration. As initial acquisition is usually achieved by a search through all possible phases (delays) of the sequence, a larger timing uncertainty means a larger search area. Beside timing uncertainty, we may also encounter frequency uncertainty which is due to Doppler shift and mismatch between the transmitter and receiver oscillators. Thus this necessitates a two-dimensional search in time and frequency. Moreover, in many cases, initial code acquisition must be accomplished in low signal-to-noise-ratio environments and in the presence of jammers. The possibility of channel fading and the existence of multiple access interference in CDMA environments can make initial acquisition even harder to accomplish.

In this chapter, we will briefly introduce techniques for initial code acquisition and code tracking for spread spectrum systems. Our focus is on synchronization techniques for DS-SS systems in a non-fading (AWGN) channel. We ignore the possibility of a two-dimensional search and assume that there is no frequency uncertainty. Hence, we only need to perform a one-dimensional search in time. Most of the techniques described in this chapter apply directly to the two-dimensional case, when both time and frequency uncertainties are present. The problem of achieving synchronization in various fading channels and CDMA environments is difficult and is currently under active investigation. In many practical systems, side information such as the time of the day and an additional control channel, is needed to help achieve synchronization.

5.1 Initial Code Acquisition

As mentioned before, the objective of initial code acquisition is to achieve a coarse synchronization between the receiver and the transmitted signal. In a DS-SS system, this is the same as matching the phase of the reference spreading signal in the despreader to the spreading sequence in the received signal. We are going to introduce several acquisition techniques which perform the phase matching just described. They are all based on the following basic working principle depicted in Figure 5.1. The receiver hypothesizes a phase of the spreading sequence and attempts to despread the received signal using the hypothesized phase. If the hypothesized phase matches the sequence in the received signal, the wide-band spread spectrum signal will be despread correctly to give a narrowband data

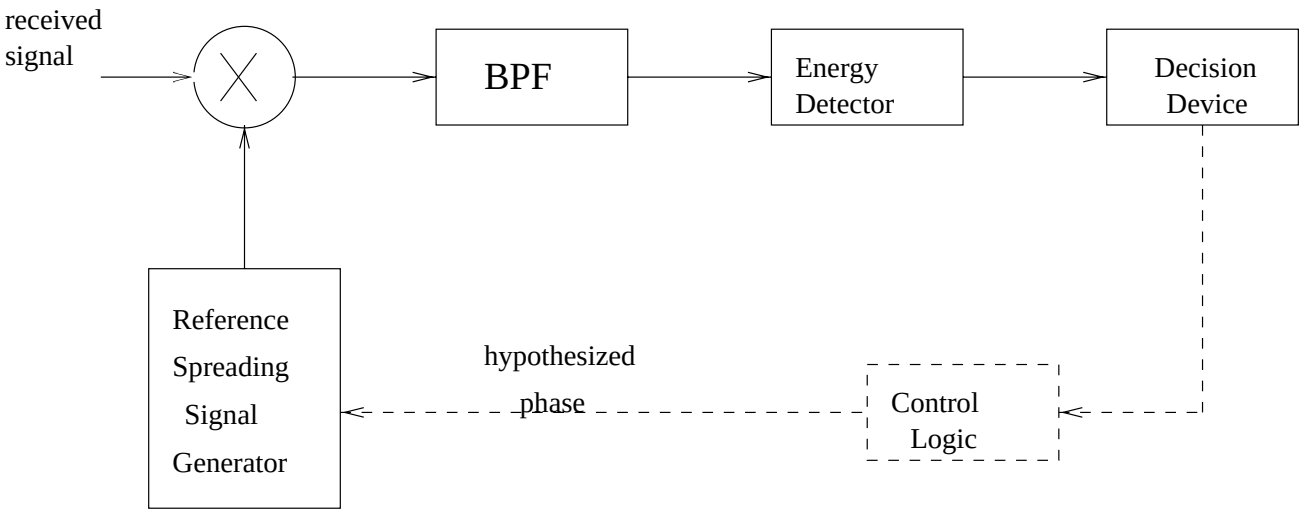

Figure 5.1: Generic acquisition circuit

signal. Then a bandpass filter, with a bandwidth similar to that of the narrowband data signal, can be employed to collect the power of the despread signal. Since the hypothesized phase matches the received signal, the BPF will collect all the power of the despread signal. In this case, the receiver decides a coarse synchronization has been achieved and activates the tracking loop to perform fine synchronization. On the other hand, if the hypothesized phase does not match the received signal, the despreader will give a wideband output and the BPF will only be able to collect a small portion of the power of the despread signal. Based on this, the receiver decides this hypothesized phase is incorrect and other phases should be tried.

We can make the qualitative argument above concrete by considering the following simplified example. We consider BPSK spreading and the transmitter spreads an all-one data sequence with a spreading signal of period T[1]. The all-one data sequence can be viewed as an initial training signal which helps to achieve synchronization. If it is long enough, we can approximately express the transmitted spread spectrum signal as $\sqrt{2P}a(t)$, where $a(t)$ is the periodic spreading signal given by

$$a(t) = \sum_{l=-\infty}^{\infty} a_l p_T(t - lT_c). \tag{5.1}$$

Neglecting the presence of thermal noise, the received signal

$$r(t) = \sqrt{2P}a(t - \Delta) \tag{5.2}$$

[1]T does not need to be the symbol duration

is just a delayed version of the transmitted signal.

Now the receiver hypothesizes a phase of the spreading sequence to generate a reference signal $a(t-\hat{\Delta})$ for despreading. The despread signal is $\sqrt{2P}a(t-\Delta)a(t-\hat{\Delta})$. Since only coarse synchronization is needed, we limit $\hat{\Delta}$ to be an integer multiple of the chip duration T_c. We integrate the despread signal for T seconds and use the square of the magnitude of the integrator output as our decision statistic. The integrator acts as the BPF and the energy detector in Figure 5.1. More precisely, the decision statistic is given by

$$\begin{aligned} z &= \frac{1}{2T^2}\left|\int_T \sqrt{2P}a(t-\Delta)a(t-\hat{\Delta})dt\right|^2 \\ &= \frac{P}{T^2}\left|r_{a,a}(\Delta-\hat{\Delta})\right|^2, \end{aligned} \tag{5.3}$$

where $r_{a,a}(\tau)$ is the continuous-time periodic autocorrelation (see (3.4)) function of the spreading signal $a(t)$. We note that $r_{a,a}(0)=T$ and with a properly chosen spreading sequence, the values of $|r_{a,a}(\tau)|$ for $|\tau|\geq T_c$ should be much smaller than T. For example, if an m-sequence of period N ($T=NT_c$) is used, then

$$r_{a,a}(\tau)=\begin{cases} T-(N+1)|\tau| & \text{for } |\tau|<T_c \\ -T_c & \text{for } |\tau|\geq T_c. \end{cases} \tag{5.4}$$

Thus, if we set the decision threshold γ to $\left(\frac{N-1}{N}\right)^2\frac{P}{2}$ and decide we have a match if $z\geq\gamma$, then we can determine Δ, by testing all possible hypothesized values of $\hat{\Delta}$, up to an accuracy of $\pm T_c/2$.

The type of energy detecting scheme considered in the above example is called the *matched filter energy detector* since the combination of the despreader and the integrator is basically an implementation of the matched filter for the spreading signal. There also exists another form of energy detector called the *radiometer* which is shown in Figure 5.2. As before, the receiver hypothesizes a phase of the spreading process. The despread signal is bandpass filtered with a bandwidth roughly equal to that of the narrowband data signal. The output of the bandpass filter is squared and integrated for a duration of T_d [2] to detect the energy of the despread signal.

The comparison between the matched filter energy detector and the radiometer brings out several important design issues for initial code acquisition circuits. The first one is the time needed to evaluate

[2] We note that T_d does not need to be the period T of the spreading signal.

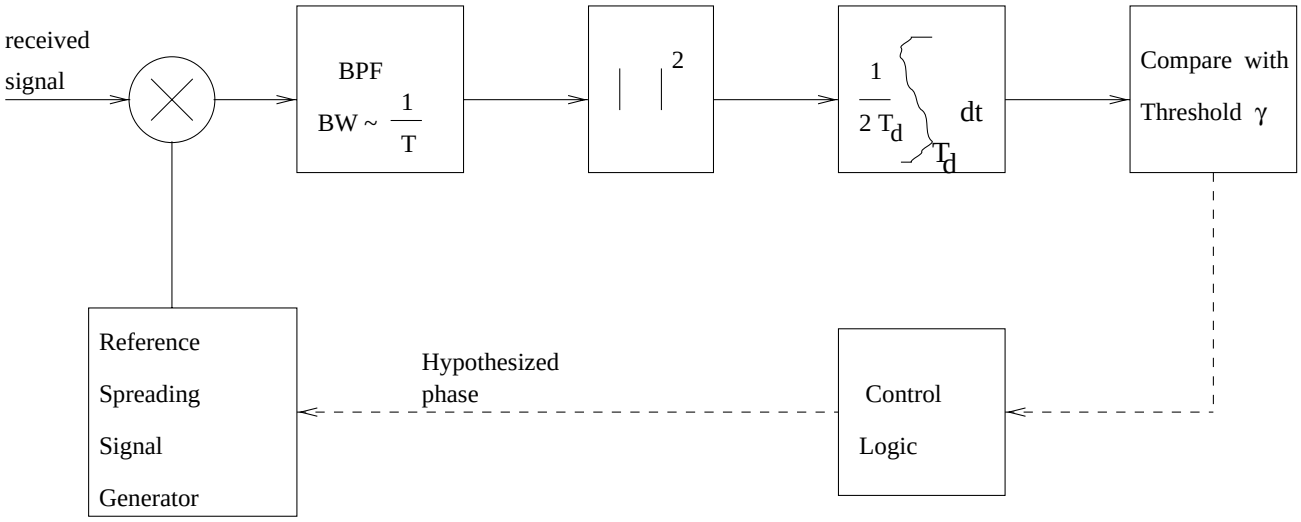

Figure 5.2: Acquisition circuit using a radiometer

a single hypothesized phase of the spreading sequence. This time is usually referred to as the *dwell time*. Neglecting the processing time for the other components in the acquisition circuit, the dwell time for the matched filter energy detector and the radiometer are determined by the integration times of the respective integrators in the matched filter energy detector and the radiometer. From the discussion above, the dwell times for the matched filter energy detector and the radiometer are T and T_d, respectively. In practice, we would like the dwell time to be as small as possible. For the matched filter energy detector, we cannot significantly reduce the integration time since the spreading sequence is usually designed to have a small out-of-phase autocorrelation magnitude, but the out-of-phase partial autocorrelation magnitude is not guaranteed to be small in standard sequence design methods. If we reduce the integration time significantly, the decision statistic would not be a function of the autocorrelation function as in (5.3), but rather a function of the partial autocorrelation function of the spreading sequence. Hence it would be difficult to distinguish whether or not we have a match between the hypothesized phase and the received signal, when noise is present. On the other hand, since the radiometer uses the BPF directly to detect whether there is a match or not and the integrator is simply employed to collect energy, we do not need to integrate for the whole period of the sequence as long as we have enough energy. The integration time and hence the dwell time can be smaller than T, provided that the BPF can settle to its steady state output in a much shorter duration than T.

Another design issue, which is neglected in the simplified example before, is the effect of noise.

The presence of noise causes two different kinds of errors in the acquisition process:

1. A *false alarm* occurs when the integrator output exceeds the threshold for an incorrect hypothesized phase.

2. A *miss* occurs when the integrator output falls below the threshold for a correct hypothesized phase.

A false alarm will cause an incorrect phase to be passed to the code tracking loop which, as a result, will not be able to lock on to the DS-SS signal and will return the control back to the acquisition circuitry eventually. However, this process will impose severe time penalty to the overall acquisition time. On the other hand, a miss will cause the acquisition circuitry to neglect the current correct hypothesized phase. Therefore a correct acquisition will not be achieved until the next correct hypothesized phase comes around. The time penalty of a miss depends on acquisition strategy. In general, we would like to design the acquisition circuitry to minimize both the false alarm and miss probabilities by properly selecting the decision threshold and the integration time. Since the integrators in both the matched filter energy detector and the radiometer act to collect signal energy as well as to average out noise, a longer integration time implies smaller false alarm and miss probabilities. We note that because of the reason indicated before, we can only increase the integration time of the matched filter energy detector in multiples of T. No such restriction is imposed on the radiometer.

Summarizing the discussions so far, we need to design the dwell time (the integration time) of the acquisition circuitry to achieve a compromise between a small overall acquisition time and small false alarm and miss probabilities. Another important practical consideration is the complexity of the acquisition circuitry. Obviously, there is no use of designing an acquisition circuit which is too complex to build.

There are usually two major design approaches for initial code acquisition. The first approach is to minimize the overall acquisition time given a predetermined tolerance on the false alarm and miss probabilities. The second approach is to associate penalty times with false alarms and misses in the calculation and minimization of the overall acquisition time. In applying each of the two approaches, we need to consider any practical constraint which might impose a limit on the complexity of the acquisition circuitry. With all these considerations in mind, we will discuss several common acquisition strategies and compare them in terms of complexity and acquisition time.

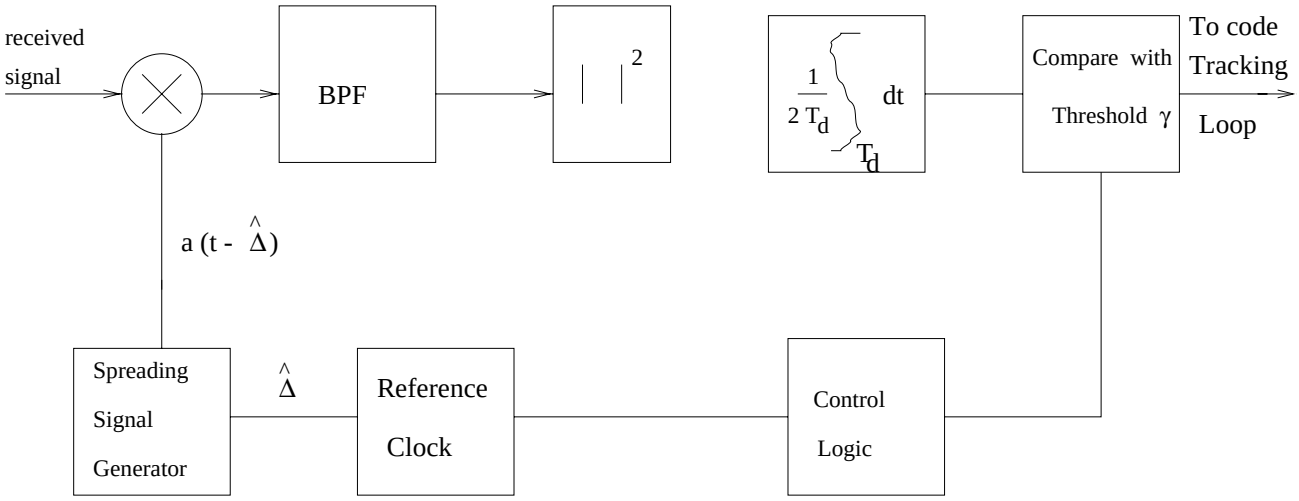

Figure 5.3: Serial search circuit

5.1.1 Acquisition strategies

Serial search

The first acquisition strategy we consider is *serial search*. In this method, the acquisition circuit attempts to cycle through and test all possible phases one by one (serially) as shown in Figure 5.3. The circuit complexity for serial search is low. However, penalty time associated with a miss is large[3]. Therefore we need to select a larger integration (dwell) time to reduce the miss probability. This, together with the serial searching nature, gives a large overall acquisition time (i.e., slow acquisition).

Parallel search

Unlike serial search, we test all the possible phases simultaneously in the parallel search strategy as shown in Figure 5.4. Obviously, the circuit complexity of the parallel search is high. The overall acquisition time is much smaller than that of the serial search.

Multidwell detection

Since the penalty time associated with a false alarm is large, we usually set the decision threshold γ in the serial search circuitry to a high value to make the false alarm probability small. However,

[3]The penalty time associated with a false alarm is always large.

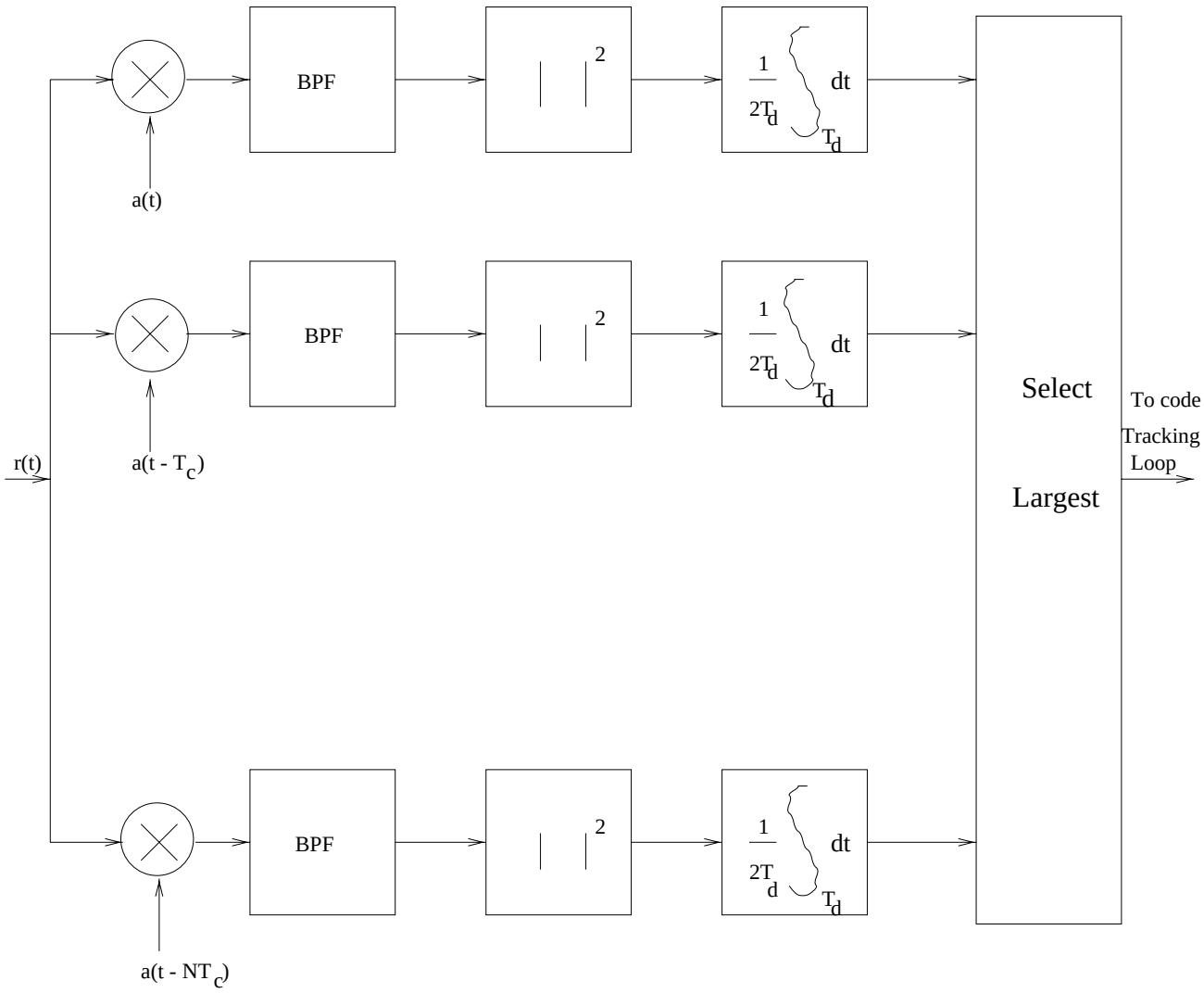

Figure 5.4: Parallel Search Circuit

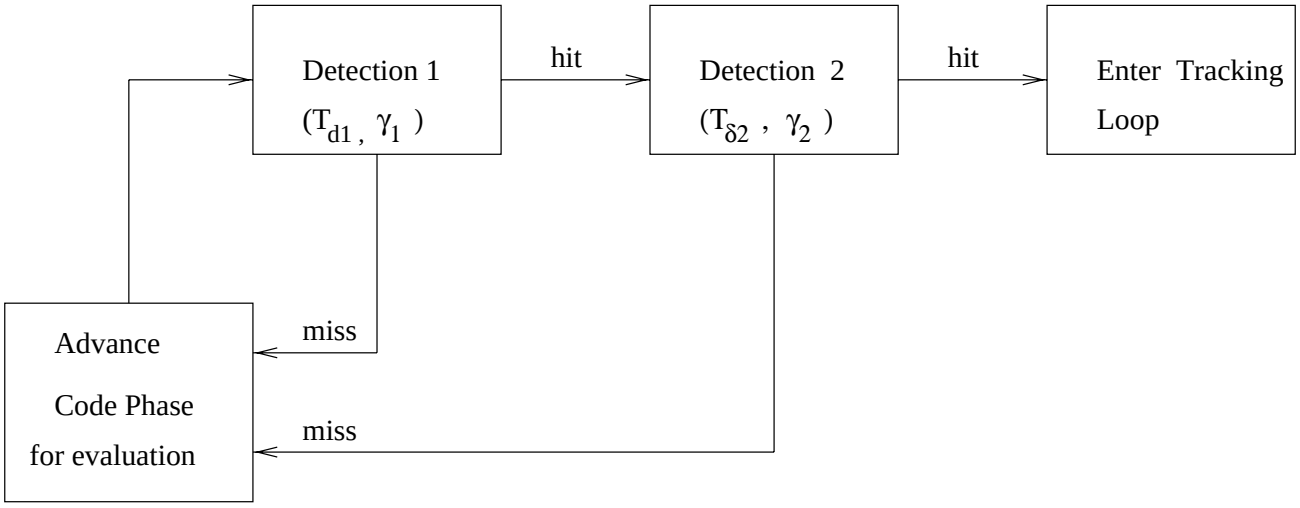

Figure 5.5: Multidwell detection flow diagram

this requires us to increase integration time T_d to reduce the miss probability since the penalty time associated with a miss is also large. As a result, the overall acquisition time needed for the serial search is inherently large. This is the limitation of using a single detection stage.

A common approach to reduce the overall acquisition the overall acquisition time is to employ a two-stage detection scheme as shown in Figure 5.5. Each detection stage in Figure 5.5 represents a radiometer with the integration time and decision threshold shown. The first detection stage is designed to have a low threshold and a short integration time such that the miss probability is small but the false alarm probability is high. The second stage is designed to have small miss and false alarm probabilities. With this configuration, the first stage can reject incorrect phases rapidly and second stage, which is entered occasionally, verifies the decisions made by the first stage to reduce the false alarm probability. By properly choosing the integration times and decision thresholds in the two detection stage, the overall acquisition time can be significantly reduced.

This idea can be extended easily to include cases where more than two decision stages are employed to further reduce the overall acquisition time. This type of acquisition strategy is called *multidwell detection*. We note that the multidwell detection strategy can be interpreted as a serial search with variable integration (dwell) time.

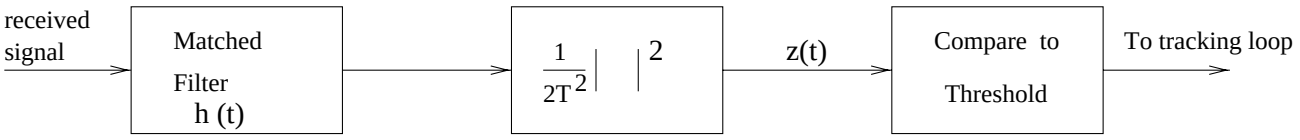

Figure 5.6: Matched filter acquisition circuit

Matched filter acquisition

Another efficient way to perform acquisition is to employ a matched filter that is matched to the spreading signal as shown in Figure 5.6. Neglecting the presence of noise, assume the received signal $r(t)$ is given by (5.2). It is easy to see that the impulse response of the matched filter is $h(t) = a^*(T-t)p_T(t)$, where $a(t)$ is the spreading signal of period T. Neglecting the presence of noise, the square of the magnitude of the matched filter output is

$$\begin{aligned} z(t) &= \frac{1}{T^2}\left|\int_{-\infty}^{\infty} r(\tau)h(t-\tau)d\tau\right|^2 \\ &= \frac{P}{T^2}\left|r_{a,a}(\Delta-(t-T))\right|^2 . \end{aligned} \tag{5.5}$$

We note that this is exactly the matched filter energy detector output with hypothesized phase $(t-T)$ (cf. (5.3)). Thus, by continuously observing the matched filter output and comparing it to a threshold, we effectively evaluate different hypothesized phases using the matched filter energy detector. The effective dwell time for a hypothesized phase is the chip duration T_c. Hence the overall acquisition time required is much shorter than that of the serial search. However, the performance of the matched filter acquisition technique is severely limited by the presence of frequency uncertainty. As a result, matched filter acquisition can only be employed in situations where the frequency uncertainty is very small.

5.1.2 False alarm and miss probabilities

As mentioned before, the presence of noise causes misses and false alarms in the code acquisition process. The false alarm and miss probabilities are the major design parameters of an acquisition technique. In this section, we present a simple approximate analysis on the false alarm and miss probabilities for the matched filter energy detector and the radiometer on which all the previously discussed acquisition strategies are based.

For simplicity, we assume only AWGN, $n(t)$, with power spectral density N_0 is present. The received signal is given by

$$r(t) = \sqrt{2P}a(t-\Delta) + n(t), \tag{5.6}$$

where $a(t)$ is the spreading signal of period T.

Matched filter energy detector

First, let us consider the matched filter energy detector. Similar to (5.3), the decision statistic z in this case is

$$\begin{aligned} z &= \frac{1}{2T^2}\left|\int_T r(t)a(t-\hat{\Delta})dt\right|^2 \\ &= \frac{1}{2T^2}\left|\int_T \sqrt{2P}a(t-\Delta)a(t-\hat{\Delta})dt + \int_T n(t)a(t-\hat{\Delta})dt\right|^2 \\ &= \left|\frac{\sqrt{P}}{T}r_{a,a}(\Delta-\hat{\Delta}) + n_z\right|^2, \end{aligned} \tag{5.7}$$

where

$$n_z = \frac{1}{\sqrt{2}T}\int_T n(t)a(t-\hat{\Delta})dt \tag{5.8}$$

is a zero-mean complex symmetric Gaussian random variable with variance $\frac{N_0}{2T}$. We test z against the threshold γ. If $z > \gamma$, we decide the hypothesized code phase $\hat{\Delta}$ matches the actual phase Δ. If $z \leq \gamma$, we decide otherwise. The step just described defines a decision rule for solving the following hypothesis-testing problem (i.e., to decide between the two hypotheses below):

H_0 : the hypothesized code phase $\hat{\Delta}$ does not match the actual phase Δ;

H_1 : the hypothesized code phase $\hat{\Delta}$ matches the actual phase Δ.

For simplicity, we assume that, under H_0, the signal contribution in the decision statistic is zero. This is a reasonable approximation since the spreading sequence is usually designed to have a small out-of-phase autocorrelation magnitude. Then, from (5.7), it is easy to see that under the two hypotheses:

$$H_0 : z = |n_z|^2, \tag{5.9}$$

$$H_1 : z = \left|\sqrt{P} + n_z\right|^2. \tag{5.10}$$

Recall that a false alarm results when we decide $\hat{\Delta}$ matches Δ (H_1) but $\hat{\Delta}$ actually does not match Δ (H_0). From (5.9), the false alarm probability, P_{fa}, is given by

$$P_{fa} = \Pr(z > \gamma | H_0) = 1 - F_{z|H_0}(\gamma), \tag{5.11}$$

where $F_{z|H_0}(\cdot)$ is the cumulative distribution function of z under H_0. Similarly, a miss results when we decide $\hat{\Delta}$ does not match Δ (H_0) but $\hat{\Delta}$ actually matches Δ (H_1). From (5.10), the miss probability, P_m, is given by

$$P_m = \Pr(z \leq \gamma | H_1) = F_{z|H_1}(\gamma), \tag{5.12}$$

where $F_{z|H_1}(\cdot)$ is the cumulative distribution function of z under H_1.

Under H_0, z is central chi-square distributed with two degrees of freedom [1] and

$$P_{fa} = 1 - F_{z|H_0}(\gamma) = \exp\left(-\frac{\gamma T}{N_0}\right). \tag{5.13}$$

Under H_1, z is non-central chi-square distributed with two degrees of freedom [1] and

$$\begin{aligned} P_m &= F_{z|H_1}(\gamma) \\ &= \int_0^{\gamma} \frac{T}{N_0} \exp\left(-\frac{u+P}{N_0/T}\right) I_0\left(\frac{\sqrt{Pu}}{N_0/2T}\right) du \\ &= \int_0^{\sqrt{2\gamma T/N_0}} u \exp\left(-\frac{u^2+2s^2}{2}\right) I_0(\sqrt{2}su) du, \end{aligned} \tag{5.14}$$

where $s^2 = PT/N_0$ is the signal-to-noise ratio (SNR) and $I_0(\cdot)$ is the zeroth order modified Bessel function of the first kind. Using (5.13) and (5.14), we can obtain the receiver operating characteristic (ROC) diagram, which is a plot showing the relationship between the detection probability P_d and the false alarm probability, of the matched filter energy detector. The relationship between P_{fa} and P_d is

$$P_d = 1 - P_m = Q\left(\sqrt{2}s, \sqrt{-2\ln P_{fa}}\right), \tag{5.15}$$

where

$$Q(\alpha, \tau) = \int_{\tau}^{\infty} u \exp\left(-\frac{u^2+\alpha^2}{2}\right) I_0(\alpha u) du \tag{5.16}$$

is the Marcum's Q-function. The ROC curves of the matched filter energy detector for different SNR's are plotted in Figure 5.7. The ROC curves indicate the tradeoff between false alarm and detection probability at different SNR's. Generally, the more "concave" the ROC curve, the better is the performance of the detector.

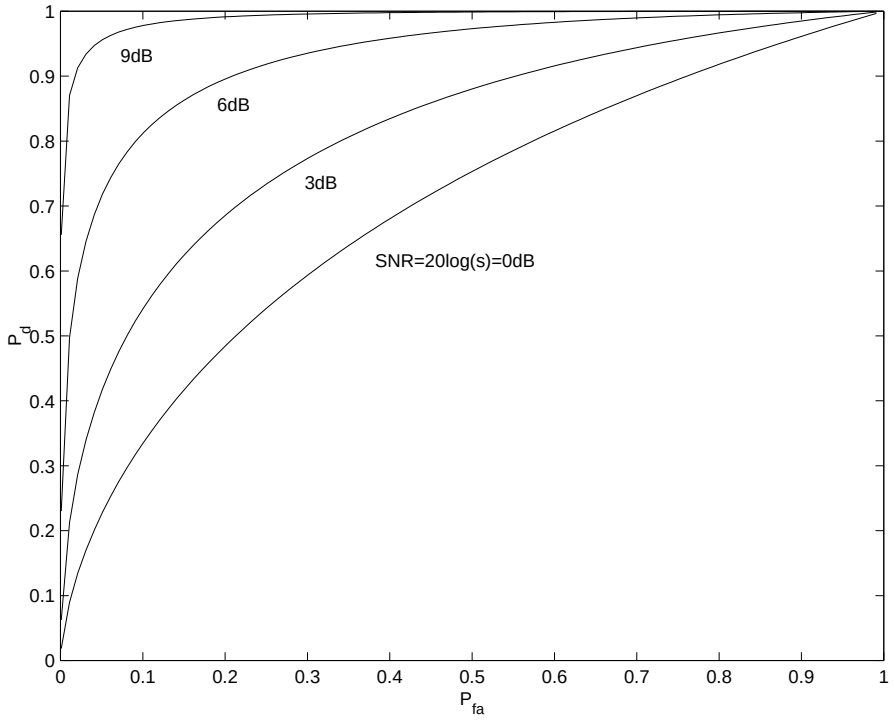

Figure 5.7: ROC's of the matched filter energy detector

Radiometer

Now, let us consider the radiometer and calculate its miss and false alarm probabilities. From Figure 5.2, the decision statistic is given by

$$\begin{aligned} z &= \frac{1}{2T_d}\int_0^{T_d} \left|L_B[r(t)a^*(t-\hat{\Delta})]\right|^2 dt \\ &= \frac{1}{2T_d}\int_0^{T_d} \left|L_B[\sqrt{2P}a(t-\Delta)a^*(t-\hat{\Delta})] + L_B[n(t)a^*(t-\hat{\Delta})]\right|^2 dt, \end{aligned} \tag{5.17}$$

where $\hat{\Delta}$ is the hypothesized phase and L_B represents the ideal low pass filter with passband $[-B/2, B/2]$ with $B \ll 1/T_c$. When the hypothesized phase matches the actual phase, i.e., $\hat{\Delta} = \Delta$, $a(t-\Delta)a^*(t-\hat{\Delta})$ is a constant signal and hence all its power passes through the lowpass filter L_B. On the other hand, when $\hat{\Delta} \neq \Delta$, $a(t-\Delta)a^*(t-\hat{\Delta})$ is a wideband signal whose bandwidth is of the order of $1/T_c$. Hence, only a very small portion of its power passes through L_B. For simplicity, we assume that the lowpass filter output due to the signal is 0 when $\hat{\Delta} \neq \Delta$. Moreover, since $B \ll 1/T_c$, we can approximate $L_B[n(t)a^*(t-\hat{\Delta})] = n'(t)$ as a zero-mean complex Gaussian random process with power spectral

density $\Phi_{n'}(f) = N_0$ for $|f| < B/2$ and $\Phi_{n'}(f) = 0$ otherwise. With these two approximations, the two hypotheses H_0 and H_1 defined previously become:

$$H_0 \quad : \quad z = \frac{1}{2T_d} \int_0^{T_d} |n'(t)|^2 dt, \tag{5.18}$$

$$H_1 \quad : \quad z = \frac{1}{2T_d} \int_0^{T_d} |\sqrt{2P} + n'(t)|^2 dt. \tag{5.19}$$

Again, if $z > \gamma$, we decide H_1. If $z \leq \gamma$, we decide H_0. As in the case of the matched filter energy detector, the false alarm and miss probabilities are given by (5.11) and (5.12), respectively. Here we need to determine the cumulative distribution function of z under H_0 and H_1 given in (5.18) and (5.19), respectively. Since the exact distributions of z under H_0 and H_1 in this case are difficult to find, we resort to approximations for simplicity. We note that the forms of z in (5.18) and (5.19) hint that z is roughly the sum of a large number of random variables under each hypothesis. Therefore, we can approximate z as Gaussian distributed. More details of this approximation can be found in [2]. With this Gaussian approximation, we only need to determine the means and variances of z under both H_0 and H_1. It can be shown (see Homework 5) that if $BT_d \gg 1$, we have approximately,

$$\mathrm{E}(z|H_0) = N_0 B, \tag{5.20}$$

$$\mathrm{E}(z|H_1) = P + N_0 B, \tag{5.21}$$

$$\mathrm{var}(z|H_0) = {N_0}^2 B/T_d, \tag{5.22}$$

$$\mathrm{var}(z|H_1) = (2PN_0 + {N_0}^2 B)/T_d. \tag{5.23}$$

Then,

$$\begin{aligned} P_{fa} &= 1 - F_{z|H_0}(\gamma) \\ &= Q\left(\frac{\gamma - N_0 B}{\sqrt{{N_0}^2 B/T_d}}\right) \\ &= Q\left(\sqrt{BT_d}\left[\frac{\gamma}{N_0 B} - 1\right]\right) \end{aligned} \tag{5.24}$$

and

$$\begin{aligned} P_d &= 1 - P_m \\ &= 1 - F_{z|H_1}(\gamma) \end{aligned}$$

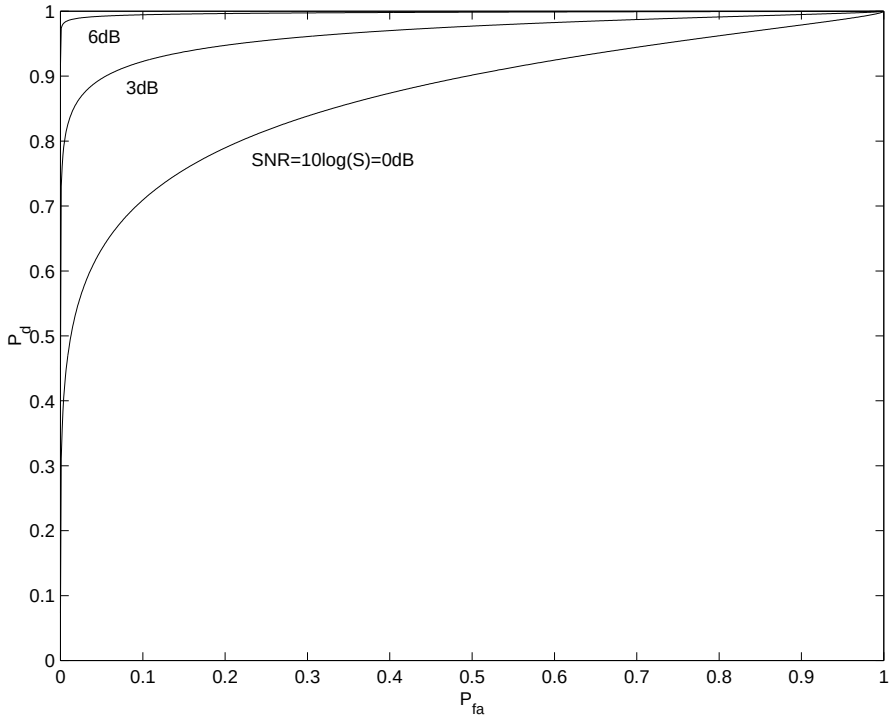

Figure 5.8: ROC's of the radiometer

$$\begin{aligned} &= Q\left(\frac{\gamma - P - N_0 B}{\sqrt{(2PN_0 + {N_0}^2 B)/T_d}}\right) \\ &= Q\left(\sqrt{\frac{BT_d}{2S+1}}\left[\frac{\gamma}{N_0 B} - (S+1)\right]\right), \end{aligned} \tag{5.25}$$

where $S = P/(N_0 B)$ is the signal-to-noise ratio. From (5.24) and (5.25), we can obtain the ROC of the radiometer:

$$P_d = Q\left(\frac{Q^{-1}(P_{fa}) - S\sqrt{BT_d}}{\sqrt{2S+1}}\right). \tag{5.26}$$

The ROC curves for $BT_d = 5$ with different values of S are plotted in Figure 5.8.

From (5.24) and (5.25), if the threshold γ is chosen so that $N_0 B < \gamma < P + N_0 B$, we can always decrease both the false alarm and miss probabilities by increasing the integration time T_d. Moreover, we have assumed that $BT_d \gg 1$. Besides simplifying the expressions in (5.20)–(5.23), this assumption is also practically motivated. If the bandwidth B of the BPF is reduced, it will take longer for its output to settle to the steady state value and hence we need to integrate the output for a longer time (i.e., larger T_d). As a result, the product BT_d still needs to be large. Of course, the overall choices

of B and T_d should be a compromise between performance and dwell time. The usual design steps for the radiometer are as follows:

1. Consult the set of ROC curves to determine all possible pairs of values for BT_d and $S = P/(N_0B)$ that give the predetermined performance for the false alarm and detection probabilities.

2. Based on a predetermined received power to noise level P/N_0, determine the values of B and T_d corresponding to each of the pair BT_d and S selected in the previous step.

3. Choose the pair B and T_d that give the best compromise between dwell time and implementation complexity.

4. Determine the threshold γ using (5.24).

Finally, we note that in the derivations of the false alarm and miss probabilities above, we have assumed that under H_1 the hypothesized phase $\hat{\Delta} = \Delta$. However, since the goal of the initial acquisition process is to achieve a coarse synchronization, we usually increase the hypothesized phase in steps. For example, $\hat{\Delta} = nT_c$. Hence, it is rarely that any of the hypothesized phases we test will be exactly equal to the correct phase. The analysis above can be slightly modified to accommodate this fact by replacing the received power P by the effective received power $Pr_{a,a}^2(\Delta - \hat{\Delta})/T^2$. In practice, since we do not know Δ, we have to replace P by the worst case effective received power. For example, if $\hat{\Delta} = nT_c$, the worst case effective received power is $Pr_{a,a}^2(T_c/2)/T^2$.

5.1.3 Mean overall acquisition time for serial search

As mentioned before, one approach of initial acquisition design is to associate penalty times with false alarms and misses, and then, try to minimize the overall acquisition time, T_{acq}. We note that since T_{acq} is a random variable, a reasonable implementation of this design approach is to minimize the mean overall acquisition time $\overline{T}_{acq} = E[T_{acq}]$. In this section, we present a simple calculation of the mean overall acquisition time of a serial search circuit.

Let us assume that we cycle through and test a total of N different hypothesized phases in each search cycle until the correct phase is detected. We associate a penalty time of T_{fa} seconds ($T_{fa} \gg T_d$)

with a false alarm. The penalty time associated with a miss is NT_d, since if we encounter a miss, the correct phase cannot be detected until the next cycle. Suppose in a given realization, the correct phase is in the nth hypothesized position, there are j misses and k false alarms, the overall acquisition time is given by

$$T_{acq}(n,j,k) = nT_d + jNT_d + kT_{fa}. \tag{5.27}$$

In this realization, we note that

- number of tests performed $= n + jN$;
- number of correct phases encountered $= j + 1$;
- number of incorrect phases encountered $= n + jN - j - 1 \stackrel{\triangle}{=} K$.

Hence, the mean overall acquisition time is

$$\overline{T}_{acq} = \sum_{n=1}^{N}\sum_{j=0}^{\infty}\sum_{k=0}^{K} T_{acq}(n,j,k)P(n,j,k), \tag{5.28}$$

where

$$\begin{aligned} P(n,j,k) &= \Pr(\text{correct phase position} = n, j \text{ misses}, k \text{ false alarms}) \\ &= P(k|n,j)P(j|n)P(n) \end{aligned} \tag{5.29}$$

In (5.29),

$$\begin{aligned} P(n) &= \Pr(\text{correct phase position} = n) = \frac{1}{N} \\ P(j|n) &= \Pr(j \text{ misses} \mid \text{correct phase position} = n) = (1-P_d)^j P_d \\ P(k|n,j) &= \Pr(k \text{ false alarms} \mid \text{correct phase position} = n, j \text{ misses}) \\ &= \Pr(k \text{ false alarms out of } K \text{ positions}) \\ &= \binom{K}{k} P_{fa}^k (1-P_{fa})^{K-k}. \end{aligned}$$

As a result,

$$\begin{aligned} \overline{T}_{acq} &= \sum_{n=1}^{N}\sum_{j=0}^{\infty}\sum_{k=0}^{K} \frac{1}{N}(1-P_d)^j P_d \binom{K}{k} P_{fa}^k (1-P_{fa})^{K-k}(nT_d + NT_d + kT_{fa}) \\ &= \sum_{n=1}^{N}\sum_{j=0}^{\infty} \frac{1}{N}(1-P_d)^j P_d \sum_{k=0}^{K} P_{fa}^k (1-P_{fa})^{K-k}(nT_d + jNT_d + kT_{fa}). \end{aligned} \tag{5.30}$$

We can use the following two identities concerning the binomial distribution to evaluate the innermost summation in (5.30):

$$\sum_{k=0}^{K} \binom{K}{k} P_{fa}^k (1-P_{fa})^{K-k} = 1, \tag{5.31}$$

$$\sum_{k=0}^{K} k\binom{K}{k} P_{fa}^k (1-P_{fa})^{K-k} = KP_{fa}. \tag{5.32}$$

Then,

$$\begin{aligned} T_{acq} &= \sum_{n=1}^{N}\sum_{j=0}^{\infty} \frac{1}{N}(1-P_d)^j P_d(nT_d + jNT_d + KP_{fa}T_{fa}) \\ &= \sum_{n=1}^{N} \frac{1}{N}\sum_{j=0}^{\infty}(1-P_d)^j P_d[n(T_d + P_{fa}T_{fa}) + j(NT_d + (N-1)P_{fa}T_{fa}) - P_{fa}T_{fa}]. \end{aligned} \tag{5.33}$$

Again, we can use the following two identities concerning the geometric distribution to evaluate the inner summation in (5.33):

$$\sum_{j=0}^{\infty}(1-P_d)^j P_d = 1, \tag{5.34}$$

$$\sum_{j=0}^{\infty} j(1-P_d)^j P_d = \frac{1-P_d}{P_d}. \tag{5.35}$$

Then,

$$\begin{aligned} \overline{T}_{acq} &= \sum_{n=1}^{N} \frac{1}{N}\left\{n(T_d + P_{fa}T_{fa}) - P_{fa}T_{fa} + \left(\frac{1-P_d}{P_d}\right)[NT_d + (N-1)P_{fa}T_{fa}]\right\} \\ &= (N-1)(T_d + P_{fa}T_{fa})\left(\frac{1}{P_d} - \frac{1}{2}\right) + \frac{T_d}{P_d}. \end{aligned} \tag{5.36}$$

Given some formulae of P_{fa} and P_d in terms of T_d, γ, P, N_0, and B, we can use (5.36) to minimize $\overline{T}_{acq}$. For example, the approximate formulae of P_{fa} and P_d in (5.24) and (5.25) can be used. However, care must be taken when using these two approximate formulae. Recall that the approximate formulae (5.24) and (5.25) are valid only when $BT_d \gg 1$. Hence, they cannot be used in the minimization of $\overline{T}_{acq}$ for all ranges of γ and T_d. In order to obtain meaningful results using (5.24) and (5.25), we have to limit the range of γ and T_d. For assumption $BT_d \gg 1$ requires us to restrict T_d such that at least $T_d \geq 2/B$. Also from the discussion before, we know that when $N_0B < \gamma < P + N_0B$, we can always increase T_d to reduce P_m and P_{fa}. Therefore, it is reasonable to force γ to lie inside the

interval $[N_0B, P+N_0B]$. With these restrictions, we can use (5.24) and (5.25) to minimize (5.36). For example, let us consider the case where $N = 127, T_{fa} = 10T, B = 1/T$, and $S = P/N_0B = 2$ (3dB). We perform a two-dimensional search to find the values of $\frac{\gamma}{N_0B} \in [1, S+1]$ and $T_d \geq 2T$ that $\overline{T}_{acq}$ is minimized. The result is that $\overline{T}_{acq}$ attains a minimum value of $303T$, when $\frac{\gamma}{N_0B} = 2.25$ and $T_d = 2T$. For more accurate result, the exact formulae [2] for P_d and P_{fa} have to be used. Finally we note that the variance of the overall acquisition time can also be calculated by using a similar procedure as the one we used in obtaining $\overline{T}_{acq}$ above [2].

5.2 Code Tracking

The purpose of code tracking is to perform and maintain fine synchronization. A code tracking loop starts its operation only after initial acquisition has been achieved. Hence, we can assume that we are off by small amounts in both frequency and code phase. A common fine synchronization strategy is to design a code tracking circuitry which can track the code phase in the presence of a small frequency error. After the correct code phase is acquired by the code tracking circuitry, a standard phase lock loop (PLL) can be employed to track the carrier frequency and phase. In this section, we give a brief introduction to a common technique for code tracking, namely, the early-late gate delay-lock loop (DLL) as shown in Figure 5.9. For simplicity, let us neglect the presence of noise and let the received signal $r(t)$ be

$$r(t) = \sqrt{2P}b(t-\Delta)a(t-\Delta)\exp \mathrm{j}(\omega_0 t + \phi), \tag{5.37}$$

where $b(t)$ and $a(t)$ are the data and spreading signals, respectively, and ω_0 and ϕ are employed to model the small frequency error after the initial acquisition and the unknown carrier phase, respectively. We assume that the data signal is of constant envelope (e.g., BPSK) and the period of the spreading signal is equal to the symbol duration T. We choose the lowpass filters in Figure 5.9 to have bandwidth similar to that of the data signal. For example, we can implement the lowpass filters by sliding integrators with window width T. Let us consider the upper branch in Figure 5.9,

$$\begin{aligned} x_1(t) &= \frac{1}{2}\left|\int_{t-T}^{t} y_1(\tau)d\tau\right|^2 \\ &= \frac{1}{2}\left|\int_{t-T}^{t} r(\tau)a^*(\tau - \hat{\Delta} + \delta T_c/2)d\tau\right|^2 \end{aligned}$$

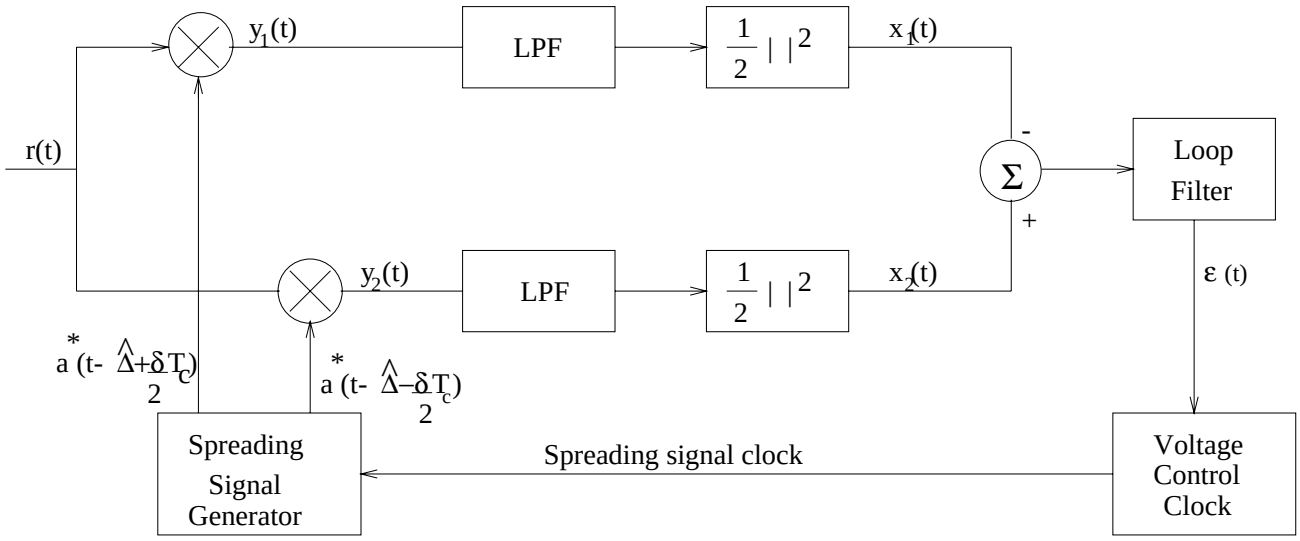

Figure 5.9: Early-late gate delay-lock loop

$$= \quad P\left|\int_{t-T}^{t} b(\tau-\Delta)a(\tau-\Delta)a^*(\tau-\hat{\Delta}+\delta T_c/2)e^{\mathrm{j}\omega_0\tau}d\tau\right|^2. \tag{5.38}$$

Since the data signal $b(t)$ is of constant envelope, the samples of the signal $x_1(t)$ at time $t = nT + \Delta$ for any integer n will be:

$$x_1(nT+\Delta) \approx P\left|r_{a,a}(\Delta-\hat{\Delta}+\delta T_c/2)\right|^2, \tag{5.39}$$

where the approximation is valid if $\omega_0 \ll 2\pi/T \approx$ bandwidth of the LPF. Between the samples, the signal $x_1(t)$ fluctuates about the constant value given in (5.39). Similarly,

$$x_2(nT+\Delta) \approx P\left|r_{a,a}(\Delta-\hat{\Delta}-\delta T_c/2)\right|^2. \tag{5.40}$$

The difference signal $x_2(t) - x_1(t)$ is then passed through the loop filter which is basically designed to output the d.c. value of its input. As a result, the error signal

$$\varepsilon(t) \approx PD_\delta\left(\frac{\Delta-\hat{\Delta}}{T_c}\right), \tag{5.41}$$

where

$$D_\delta(u) \stackrel{\triangle}{=} |r_{a,a}((u-\delta/2)T_c)|^2 - |r_{a,a}((u+\delta/2)T_c)|^2. \tag{5.42}$$

For a spreading signal based on an m-sequence of period N and rectangular chip waveform, it can be shown [2] that the function $D_\delta(x)$ takes the following form. For $\delta \geq 1$,

$$D_\delta(u) = \begin{cases} 0 & \text{for } -N+1+\frac{\delta}{2} < u \leq -\left(1+\frac{\delta}{2}\right) \\ \frac{1}{N^2} - \left[1+\left(1+\frac{1}{N}\right)\left(u+\frac{\delta}{2}\right)\right]^2 & \text{for } -\left(1+\frac{\delta}{2}\right) < u \leq -\frac{\delta}{2} \\ \frac{1}{N^2} - \left[1-\left(1+\frac{1}{N}\right)\left(u+\frac{\delta}{2}\right)\right]^2 & \text{for } -\frac{\delta}{2} < u \leq -\left(1-\frac{\delta}{2}\right) \\ 2\left(1+\frac{1}{N}\right)\left[2-(1+\frac{1}{N})\delta\right]u & \text{for } -\left(1-\frac{\delta}{2}\right) < u \leq 1-\frac{\delta}{2} \\ \left[1+\left(1+\frac{1}{N}\right)\left(u-\frac{\delta}{2}\right)\right]^2 - \frac{1}{N^2} & \text{for } 1-\frac{\delta}{2} < u \leq \frac{\delta}{2} \\ \left[1-\left(1+\frac{1}{N}\right)\left(u-\frac{\delta}{2}\right)\right]^2 - \frac{1}{N^2} & \text{for } \frac{\delta}{2} < u \leq 1+\frac{\delta}{2}, \end{cases} \tag{5.43}$$

and for $\delta \leq 1$,

$$D_\delta(u) = \begin{cases} 0 & \text{for } -N+1+\frac{\delta}{2} < u \leq -\left(1+\frac{\delta}{2}\right) \\ \frac{1}{N^2} - \left[1+\left(1+\frac{1}{N}\right)\left(u+\frac{\delta}{2}\right)\right]^2 & \text{for } -\left(1+\frac{\delta}{2}\right) < u \leq -\left(1-\frac{\delta}{2}\right) \\ -2\left(1+\frac{1}{N}\right)\delta\left[1+\left(1+\frac{1}{N}\right)u\right] & \text{for } -\left(1-\frac{\delta}{2}\right) < u \leq -\frac{\delta}{2} \\ 2\left(1+\frac{1}{N}\right)\left[2-\left(1+\frac{1}{N}\right)\delta\right]u & \text{for } -\frac{\delta}{2} < u \leq \frac{\delta}{2} \\ 2\left(1+\frac{1}{N}\right)\delta\left[1-\left(1+\frac{1}{N}\right)u\right] & \text{for } \frac{\delta}{2} < u \leq 1-\frac{\delta}{2} \\ \left[1-\left(1+\frac{1}{N}\right)\left(u-\frac{\delta}{2}\right)\right]^2 - \frac{1}{N^2} & \text{for } 1-\frac{\delta}{2} < u \leq 1+\frac{\delta}{2}. \end{cases} \tag{5.44}$$

We note that $D_\delta(u)$ is periodic with period N. Plots of $D_\delta(u)$ for different values of δ are given in Figure 5.10. From the figure, if we choose $\delta = 1$, the loop filter output will be linear with respect to the code phase error $\Delta - \hat{\Delta}$, if $|\Delta - \hat{\Delta}| \leq T_c/2$. Hence we can use the loop filter output $\varepsilon(t)$ to drive a voltage control clock which adjusts the hypothesized phase reference $\hat{\Delta}$, as depicted in Figure 5.9 to achieve fine synchronization.

5.3 References

[1] J. G. Proakis, *Digital Communications*, 3rd Ed., McGraw-Hill, Inc., 1995.

[2] R. L. Peterson, R. E. Ziemer, and D. E. Borth, *Introduction to Spread Spectrum Communications*, Prentice Hall, Inc., 1995.

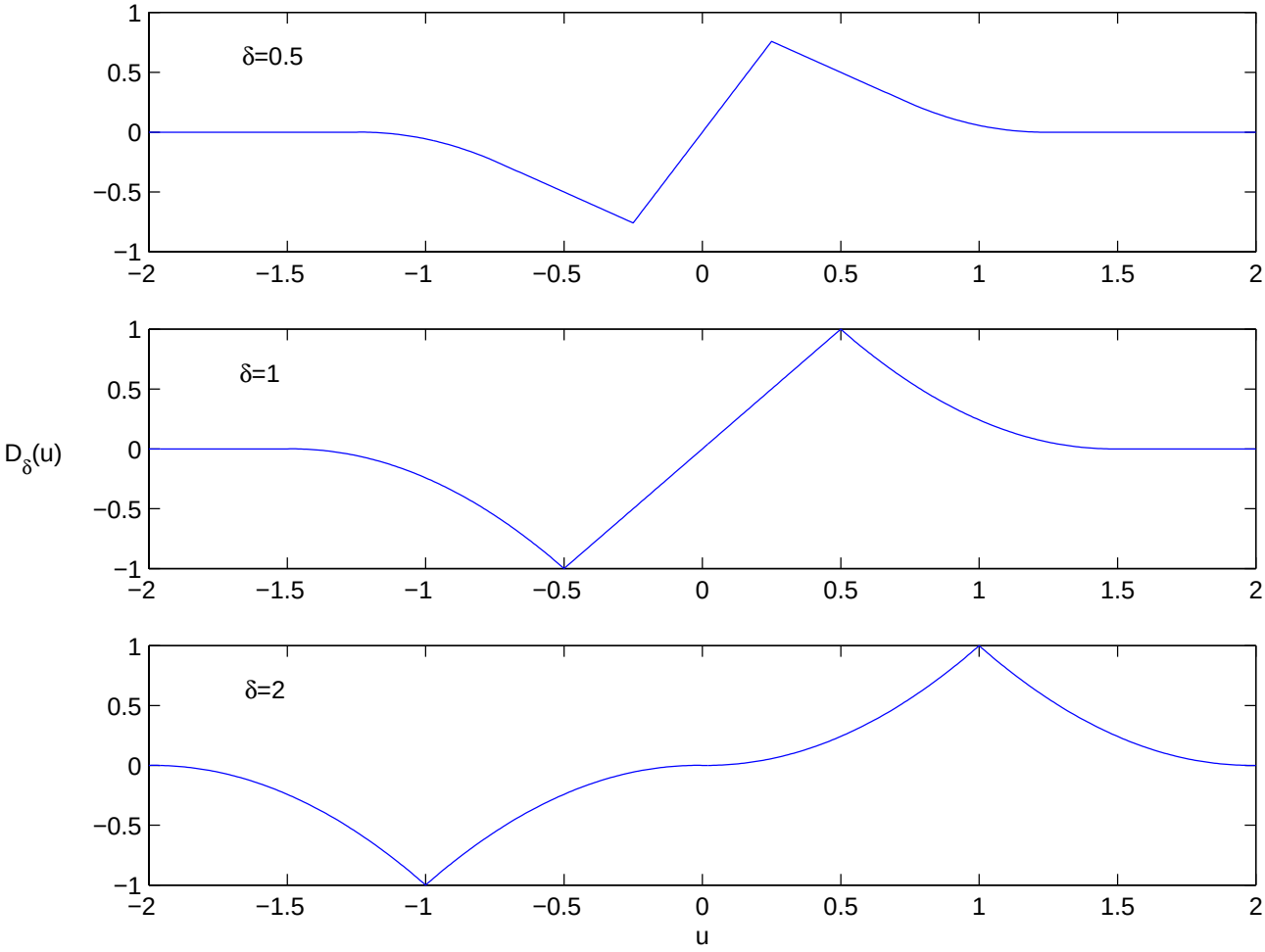

Figure 5.10: S-curves for the early-late gate delay-lock loop